doi:10.20944/preprints201911.0103.v1

Peer-reviewed version available at *Molecules* **2019**, *24*, 4274; doi:10.3390/molecules24234274

The Halogen-Bond Nature in Noble Gas-Dihalogen Complexes from Scattering Experiments and Ab-Initio Calculations

Francesca Nunzi,[a,b*] *Benedetta Di Erasmo,*[a] *Francesco Tarantelli,*[a,b] *David Cappelletti,* [a] *Fernando Pirani*[a]*

[a] Dipartimento di Chimica, Biologia e Biotecnologie, via Elce di Sotto 8, I-06123 Perugia, Italy

[b] and Istituto CNR di Scienze e Tecnologie Chimiche "Giulio Natta" (CNR-SCITEC), via Elce di Sotto, I-06123 Perugia, Italy

Corresponding Author **E-mail: francesca.nunzi@unipg.it; fernando.pirani@unipg.it*

Abstract

In order to clarify the nature of the halogen bond (XB), we considered the prototype noble gas – dihalogen molecule (Ng-X_2) systems, focusing on the nature, range and strength of the interaction. We exploited data gained from molecular beam scattering experiments with the measure of interference effects to obtain a suitable formulation of the interaction potential, with the support of high-level *ab initio* calculations, and charge displacement analysis. The essential interaction components involved in the Ng-X_2 adducts have been characterized, pointing at their critical balance in the definition of the XB. Particular emphasis is devoted to the energy stability of the orientational Ng-X_2 isomers, the barrier for the X_2 hindered rotation, and the influence of the X_2 electronic state. The present integrated study returns reliable force fields for molecular dynamics simulations in Ng-X_2 complexes that can be extended to systems with increasing complexity and whose properties depend on the selective formation of XB.

Keywords:

cross sections; molecular beam scattering; charge trasfer; coupled cluster; excited states; ionization potential; electron affinity; interaction potential; stereoselectivity

Preprints (www.preprints.org) | NOT PEER-REVIEWED | Posted: 10 November 2019 doi:10.20944/preprints201911.0103.v1

Peer-reviewed version available at Molecules 2019, 24, 4274; doi:10.3390/molecules24234274

1. Introduction

The intermolecular halogen bond (XB), the non-covalent interaction involving an electrophilic region of a halogen atom, is known to control important static and dynamic properties of matter [1]. XB role and selectivity are of high relevance in supramolecular chemistry, for the synthesis of materials with a wide variety of technological properties and drug design [2, 3]. Moreover, there are important energy transfer processes and predissociation phenomena where the chemical kinetics is guided by interaction forces associated with the XB formation [4-8].

The intermolecular interactions are usually regarded as constituted by two kinds of main contributions, that are the *electrostatic* (V_{el}) and *non-electrostatic* (V_{nel}) ones [9]. The former contribution originates from the interaction of charges and permanent electric dipoles or multipoles present in the interacting species. V_{el} is often dominating and it makes the extent and role of V_{nel}, though often important, difficult to quantify. The nature of V_{nel} is difficult to assess precisely, as it arise from the delicate balance of various components: Pauli size-repulsion (V_{sr}), dispersion (V_d) and induction (V_i) attractions, and charge-transfer (V_{ct}), which all possess different dependence and scaling properties with the distance and relative orientation of the interacting partners. In this respect, the study of simple systems with high orientational symmetry and where V_{el} is small or even vanishing is especially important to understand and model the various V_{nel} components. Noble-gas—halogen adducts, Ng—X_2 (X = Cl, Br, I) are such ideal prototypes to investigate the role of V_{nel} components in XB emergence. A recent study we carried out of the Ng—Cl_2 systems has shown, for example, that XB formation selectively stabilizes the collinear configuration of the adducts when Cl_2 is in its $X\ {}^1\Sigma_g$ ground state, while this effect disappears if Cl_2 is in its first triplet excited state, $B\ {}^3\Pi_u$ [10, 11]. We have further studied in detail how the XB formation and the charge transfer (CT) component make the interaction potential deviate from the typical van der Waals model, V_{vdW} (defined as $V_{vdW} = V_{sr} + V_d$), and how these additional components can be accurately modeled in general [10].

Peer-reviewed version available at Molecules 2019, 24, 4274; doi:10.3390/molecules24234274

In the present work, we build on our previous findings in order to characterize the entire family of the Ng—X_2 complexes. This systematic study will enable us to establish, in a consistent fashion, trends and features which govern the XB formation, its dependence on the nature of Ng and X_2, in an effort to continue the development of a general predictive model to describe the XB – in particular components other than the electrostatic one, which is of crucial importance for the design and analysis of more complex systems. As in previous works [11-14]. we use an integrated phenomenological—theoretical approach. The phenomenological procedure is based on the available data resulting from collisional experiments, combined with (semi)empirical methods developed over the years to predict range and strength of weak interactions and to provide an adequate analytical representation of the potential energy surfaces (PES). This is flanked by highly accurate theoretical *ab initio* calculations, which allow us to validate and improve the PES and the models, and to understand and characterize the fundamental components of the interaction. Key to this approach is our *ab initio* charge-displacement (CD) analysis, which enables us in particular to assess and quantify in a transparent and consistent way the elusive CT component [14].

2. Results and Discussion

2.1 Scattering results

The total integral cross section $Q(v)$ as a function of the collision velocity v have been measured by means of molecular beam technique, the noble gases He, Ne, Ar being the projectiles and the electronic ground state Cl_2 / Br_2 halogen molecules being the targets [10, 11, 15]. The results are reported in Figure 1 and clearly point out that the measured cross-section is made up of the superposition of a smooth average component and an oscillating pattern arising from the quantum “glory” interference. In particular, the cross sections are plotted as $Q(v)\cdot v^{2/5}$ to emphasize the well resolved oscillatory patterns due to the quantum interference. As is well known [16, 17], the average component is directly related to the absolute scale of the long range mean attractive interaction potential of the colliding system. Frequency, amplitude and position of the ”glory” oscillations are instead determined by the absolute value, form and anisotropy of the potential near the equilibrium configuration. On overall, the collected scattering data return direct information on the basic features of the phenomenological PES describing the intermolecular interaction in the Ng-X_2 systems. The data in Figure 1 evidence that both the smooth average and the oscillating cross section components vary along the Ng series for a selected halogen molecule and with the halogen moiety for a selected Ng, attesting to the sensitivity of the experiment to the details of the interaction.

Peer-reviewed version available at *Molecules* **2019**, *24*, 4274; doi:10.3390/molecules24234274

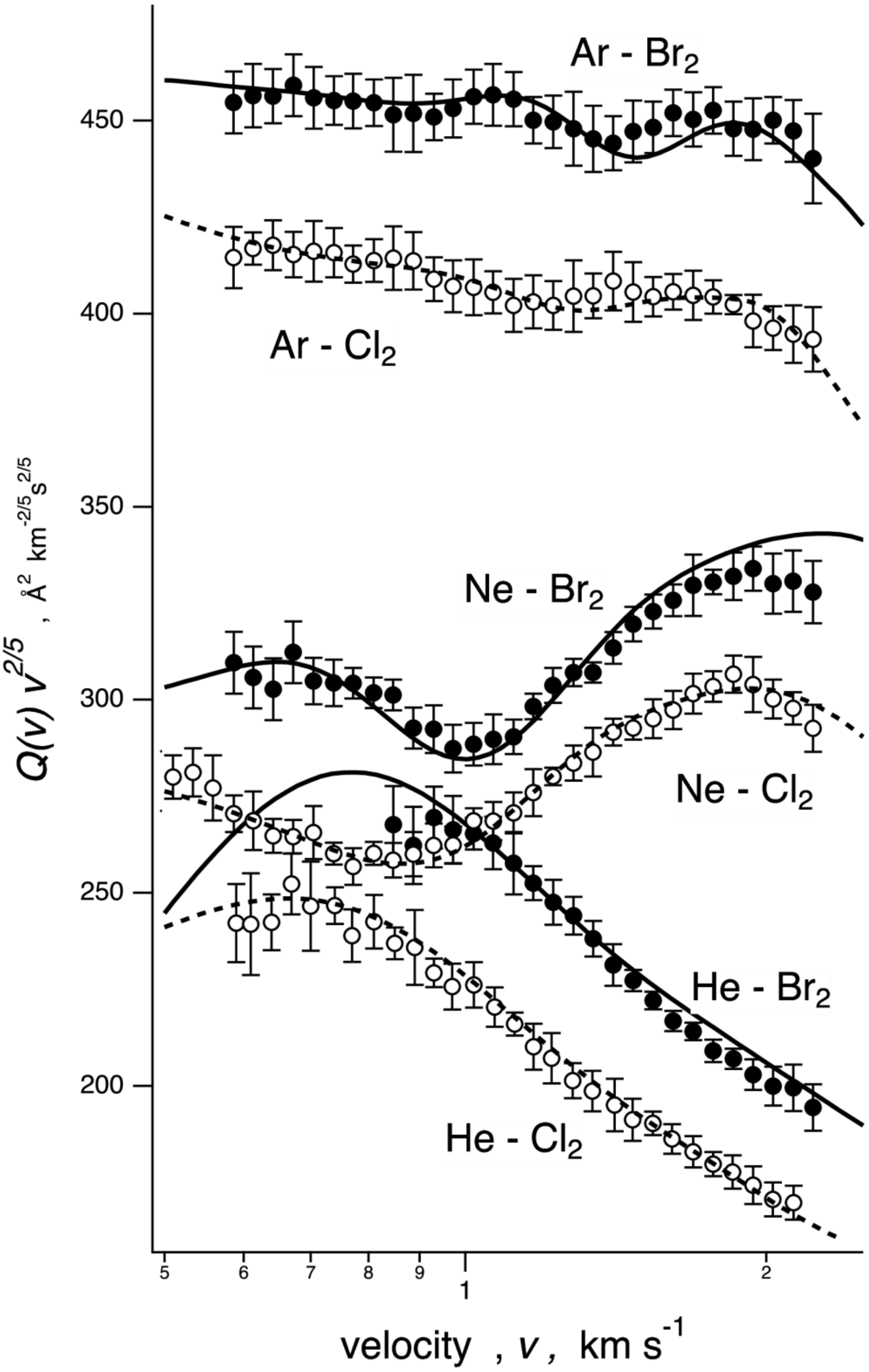

Figure 1. Integral cross sections *Q(v)* for Ng atom projectiles colliding at each selector velocity *v* with Cl_2 and Br_2 targets. The black solid lines are the best-fit cross section calculated from the model potential (see text); the dashed lines refer to the spherically component of the PESs.

Peer-reviewed version available at Molecules 2019, 24, 4274; doi:10.3390/molecules24234274

2.2 Interaction Potential Components

An analytical form of the interaction PES which in this case is expressed as a function of the vector **R** length, with **R** joining Ng and X_2 midpoint, and of the Θ angle between **R** and X_2 axis (see Figure S1 in the Supplementary Materials, SM), has been used to fit the experimental observable by tuning few physically meaningful parameters defining strength and range of the fundamental interaction components. Specifically, each PES has been defined as combination of the ubiquitous van der Waals (V_{vdW}) component, given in a suitable anisotropic form, with a three-body contribution V_{3B}, arising from the strongly asymmetric electronic charge distribution around the X_2 molecule, to which has been added the stereo-selective role of a CT stabilization effect (V_{CT}). An important test of the analytical form of the interaction potential and of its parametrization have been obtained by calculating the scattering cross sections for each system from the spherical average and from the full PESs, to reproduce, at low and high collision velocity, respectively, values and velocity dependence of measured data, including also frequency and amplitude of the oscillating patterns. In particular, results calculated under the two limiting conditions have been combined according to the different dynamical regimes, emerging in different collision velocity ranges (see refs [10, 11, 15] and below), in order to provide a better comparison with the experimental data. As it is shown in Figure 1, the employed potential model adequately reproduces cross section values and both amplitude and frequency of the glory patterns observed in the investigated Ng-X_2 systems. The potential analytical form is further validated by comparing selected cuts of the *phenomenological* PESs with the *ab initio* ones (see next sections).

When experimental cross sections data are missing, the analytical expression for the PES can be gained by merely adopting potential parameters, obtained by proper scaling laws defined in terms of fundamental physical properties of the interacting partners [10-14], and then applying the fine-tuned

Peer-reviewed version available at *Molecules* **2019**, *24*, 4274; doi:10.3390/molecules24234274

phenomenological model potential - see the Ng-X_2 complexes involving the heavier (Kr, Xe) Ngs or I_2 and/or when X_2 is in the lowest excited B state.

Further details on the PES parametrization are given in the next section. The main features of the obtained PESs, in terms of equilibrium distances R_m and interaction energy absolute values (binding energies) E_m are given in Tables 1-2 for a useful comparison of all systems. Since general and common trends have been observed among the Ng-X_2 complexes, selected values related to Ng-Br_2 and Ar-X_2 (X = Cl, Br, I) complexes are considered in Figures 2-3, showing the angular minimum energy path (MEP) associated to the PESs (see Figures S2-S5 in SM for Ng-Cl_2 and Ng-I_2 systems). For the ground state Ng-$Br_2(X)$ complexes, the Figure 2 (left side) emphasizes the increase of the interaction along the Ng series and shows the occurrence of a saddle point at intermediate orientation angle (Θ is about 50-60°). For each system the ground state linear configuration ($\Theta = 0°$) results more stable than that of the excited state (right side of Figure 2) and for heavier Ng-$Br_2(X)$ systems such configuration becomes in absolute the most stable one. In all cases a relevant selectivity arises from the different angular dependence of the interaction components involved. The various components concurring to the overall interaction potential, evaluated along the MEPs, are reported in Figure 3 for the selected Ar-$X_2(X)$ adducts (X= Cl, Br, I). Interestingly, it points out that the V_{vdW} component tends to stabilize the perpendicular configuration ($\Theta = 90°$), while the V_{CT} contribution emerges more efficiently in proximity of the collinear configuration and V_{3B} provides a less important, although repulsive, contribution at intermediate configurations. We have verified that for the excited PESs the contribution of V_{3B} and V_{CT} is found to be vanishing, suggesting that the involved interactions show a pure van der Waals behaviour. Therefore, the full topography of each PES depends on the critical balance of the effectiveness of the V_{vdW}, V_{CT} and V_{3B} components. All these peculiarities of the intermolecular interaction in Ng-X_2 complexes are confirmed by the *ab initio* calculations (see below).

Peer-reviewed version available at Molecules 2019, 24, 4274; doi:10.3390/molecules24234274

Table 1. Equilibrium distances (R_m, Å) and interaction energy absolute values (E_m, meV) of the phenomenological interaction potential considered as spherical average (V_{sph}) or in the selected linear (V_{lin}) and perpendicular (V_{perp}) orientation for the Ng-X_2 complexes in the $X\ ^1\Sigma_g$ ground state.

	V_{sph}		V_{lin}		V_{perp}	
	R_m	E_m	R_m	E_m	R_m	E_m
He-Cl$_2$	4.16	3.23	4.27	5.93	3.39	6.15
Ne-Cl$_2$	4.16	6.98	4.29	12.21	3.44	12.10
Ar-Cl$_2$	4.33	17.99	4.53	27.01	3.70	27.12
Kr-Cl$_2$	4.43	23.01	4.61	34.67	3.83	32.78
Xe-Cl$_2$	4.56	27.77	4.73	41.45	4.00	37.71
He-Br$_2$	4.41	3.24	4.51	6.51	3.50	6.43
Ne-Br$_2$	4.40	7.29	4.52	14.09	3.54	13.22
Ar-Br$_2$	4.57	18.42	4.75	30.03	3.81	29.28
Kr-Br$_2$	4.61	25.69	4.77	43.92	3.88	38.91
Xe-Br$_2$	4.73	32.24	4.86	55.02	4.04	46.18
He-I$_2$	4.85	2.76	4.95	5.54	3.79	5.54
Ne-I$_2$	4.80	6.46	4.90	13.21	3.78	12.21
Ar-I$_2$	4.88	19.20	5.04	34.66	3.94	32.98
Kr-I$_2$	4.93	26.34	5.05	49.82	4.02	43.19
Xe-I$_2$	5.02	34.64	5.11	65.77	4.16	54.26

Table 2. Equilibrium distances (R_m, Å) and interaction energy absolute values (E_m, meV) of the phenomenological interaction potential considered as spherical average (V_{sph}) or in the selected linear (V_{lin}) and perpendicular (V_{perp}) orientation for the Ng-X_2 complexes in the $B\ ^3\Pi_u$ excited state.

	V_{sph}		V_{lin}		V_{perp}	
	R_m	E_m	R_m	E_m	R_m	E_m
He-Cl_2	4.37	2.69	4.82	3.24	3.37	5.79
Ne-Cl_2	4.40	5.52	4.84	6.77	3.41	11.59
Ar-Cl_2	4.58	14.45	5.00	17.60	3.67	27.37
Kr-Cl_2	4.68	18.66	5.10	22.68	3.78	34.18
Xe-Cl_2	4.82	23.18	5.25	28.11	3.95	40.61
He-Br_2	4.57	2.67	5.03	3.15	3.61	5.37
Ne-Br_2	4.58	5.66	5.03	6.77	3.63	11.21
Ar-Br_2	4.73	16.01	5.16	19.24	3.82	29.41
Kr-Br_2	4.81	21.25	5.24	25.43	3.92	38.03
Xe-Br_2	4.93	27.14	5.35	32.51	4.07	46.35
He-I_2	5.12	2.13	5.62	2.85	3.83	4.88
Ne-I_2	5.10	4.66	5.59	6.32	3.82	10.62
Ar-I_2	5.19	14.69	5.66	20.05	3.94	31.73
Kr-I_2	5.26	20.15	5.73	27.30	4.02	42.49
Xe-I_2	5.35	26.94	5.83	36.42	4.14	55.01

Peer-reviewed version available at Molecules 2019, 24, 4274; doi:10.3390/molecules24234274

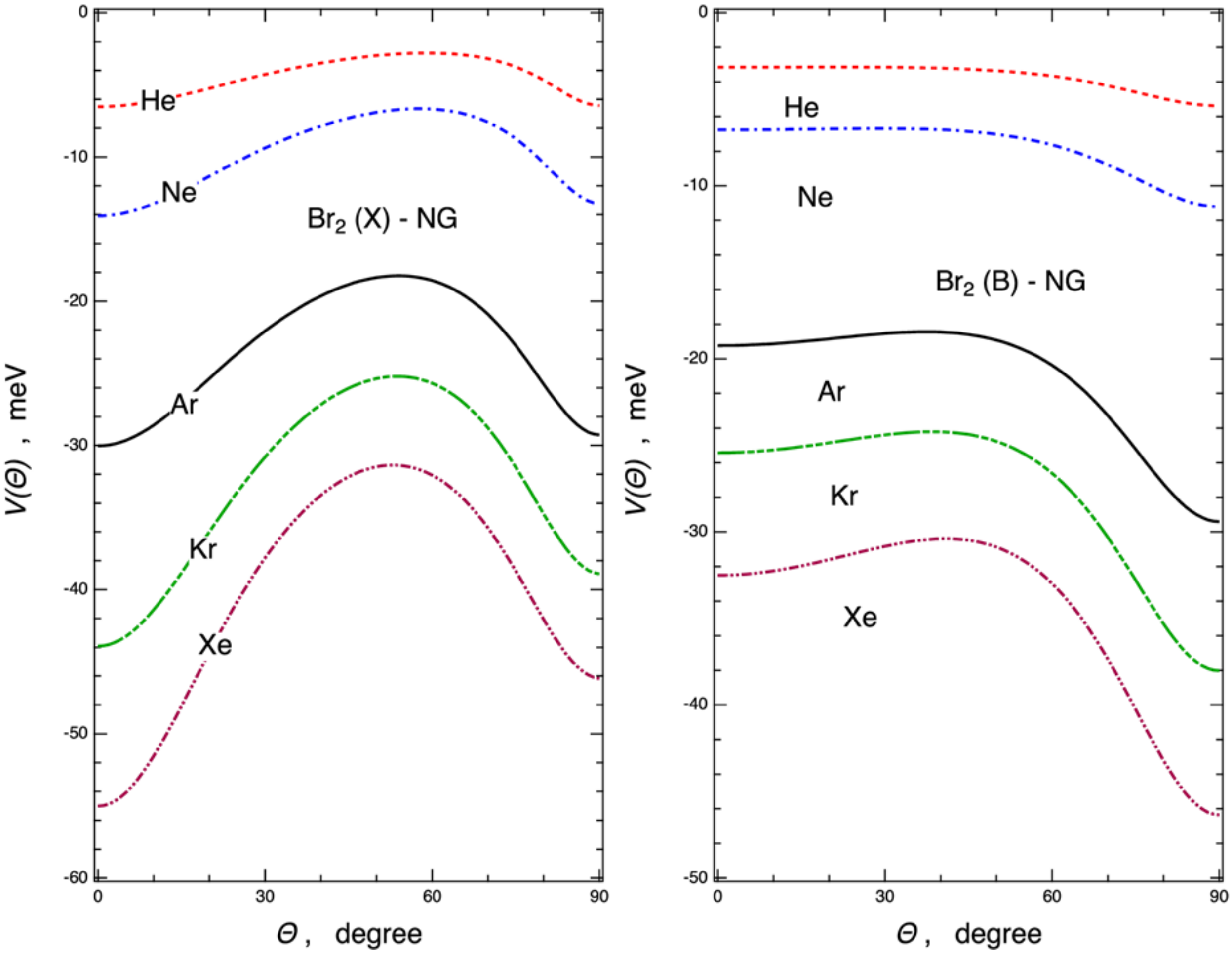

Figure 2. Angular MEP for the Ng-Br_2 complexes in the ground $X\ ^1\Sigma_g$ (left) and excited $B\ ^3\Pi_u$ (right) state of Br_2, reporting the total interaction energy V, as derived from the potential parametrization, vs the angular variable Θ.

Peer-reviewed version available at Molecules 2019, 24, 4274; doi:10.3390/molecules24234274

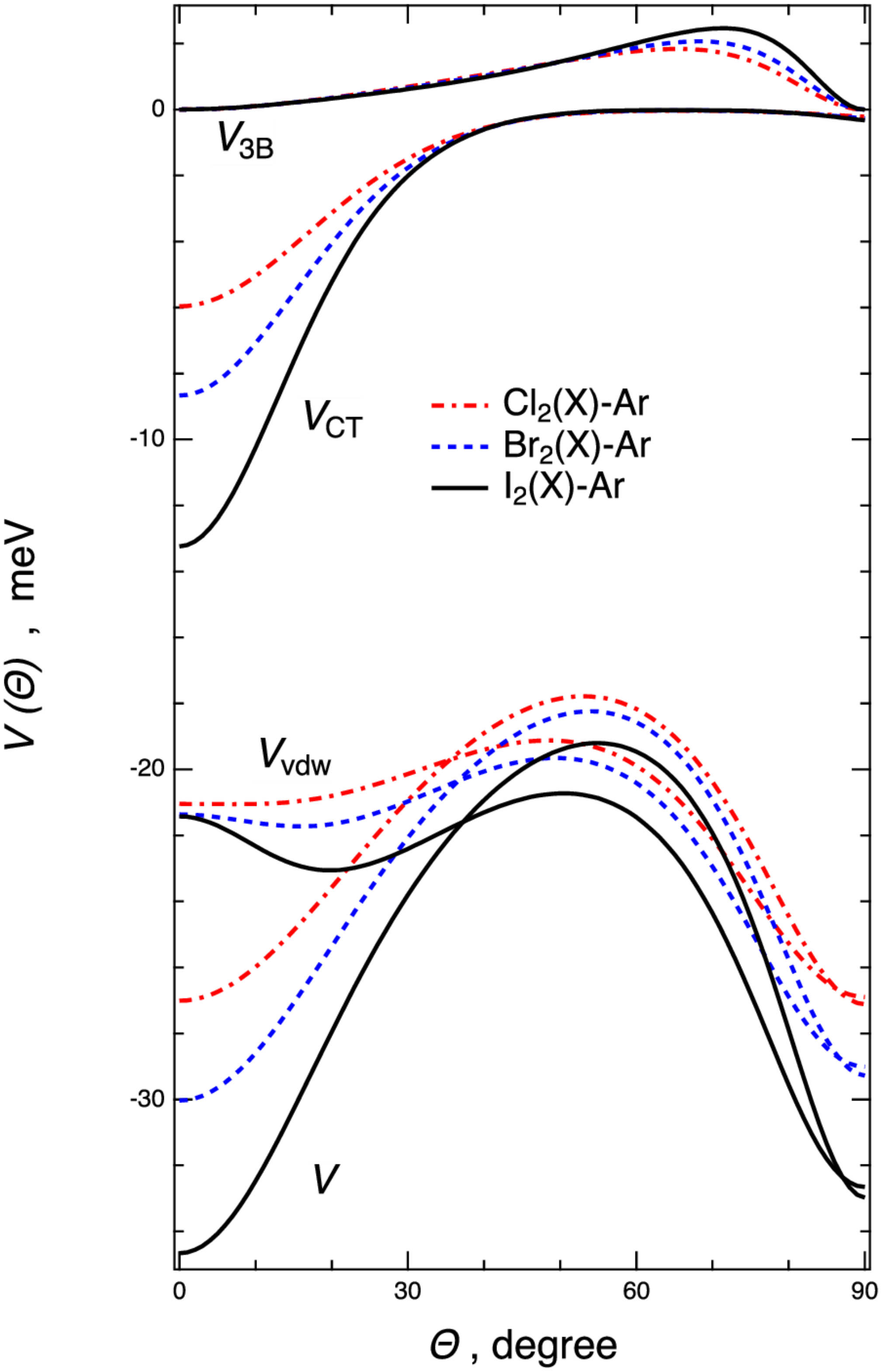

Figure 3. Angular MEP for the Ar-X_2 complexes in the ground $X\ ^1\Sigma_g$ state of X_2 (X = Cl, Br, I), reporting the overall interaction energy *V* and its components (V_{vdw}, V_{CT} and V_{3B}), as derived from the potential parametrization, vs the angular variable, *Θ*.

Peer-reviewed version available at *Molecules* **2019**, *24*, 4274; doi:10.3390/molecules24234274

2.3 *Ab initio* Potential Energy Surfaces

As discussed above, *ab initio* calculations have been performed on the Ng-X_2 adducts aimed at assessing the leading interaction components, with a particular focus on their origin in the electron density displacement, and to further test the validity of the adopted intermolecular potential formulation. We focused on the cuts of the PESs most relevant for the anisotropic behaviour of the Ng-X_2 interaction, that is the linear and the T-shaped configurations. For the saddle isomer both the *ab initio* and the phenomenological PESs return a Θ value of ca. 50-60° for all the Ng-X_2 systems. The *ab initio* computed cuts of the PES for the three considered configurations have been compared with those derived from the semi-empirical potential model parametrization, eventually fitted through the analysis of cross section data. In Figure 4 we report the *ab-initio* and model cuts of the PES for the Ar-X_2 complexes (X = Br, I) in the *X* ground state, while those for the Cl_2 adducts are reported in Reference [11]. It is clearly pointed out a satisfactory agreement (within the combined own uncertainty) between the *ab initio* and the model potentials, thus further confirming the validity of the parametrized semi-empirical model for the accurate representation of the Ng-X_2 interaction (X = Cl, Br, I) over the whole range of interaction distances, orientation angles and strengths. The optimized intermolecular distance (R_m) of the equilibrium structures and the corresponding interaction energies (E_m) of the considered cuts are reported in the SM section, Table S1.

For the selected Ar-Br_2 adduct, we also report in Figure 5 the computed cuts of the electronically excited PES, compared with those provided by the phenomenological potential model. Here too, the agreement is entirely satisfactory. The interpretation afforded by the model reveals that, at variance with the ground state, the interaction in the excited state is entirely of van der Waals nature, thus explaining the higher energy stability of the T-shaped vs linear configuration, the V_{CT} and V_{3B} components playing a minor role.

Peer-reviewed version available at *Molecules* **2019**, *24*, 4274; doi:10.3390/molecules24234274

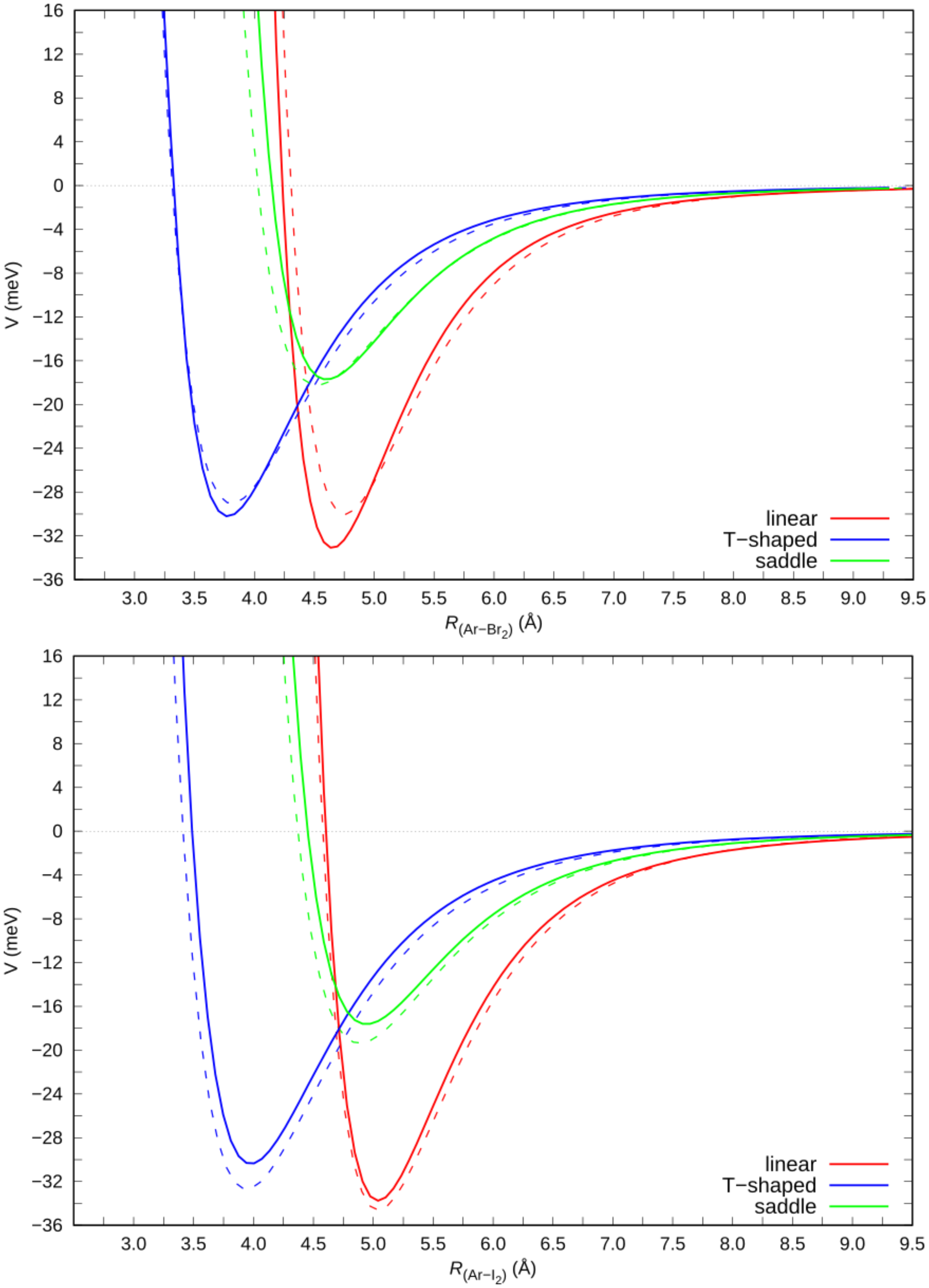

Figure 4. Solid lines: potential energy curves (interaction potential V vs Ar-X_2 distance R) for Ar-Br_2 (top, CCSD(T)/AV5Z) and Ar-I_2 (bottom, CCSD(T)/AVQZ) in their ground state. Dashed lines: corresponding curves obtained from the semi-empirical model.

Peer-reviewed version available at Molecules 2019, 24, 4274; doi:10.3390/molecules24234274

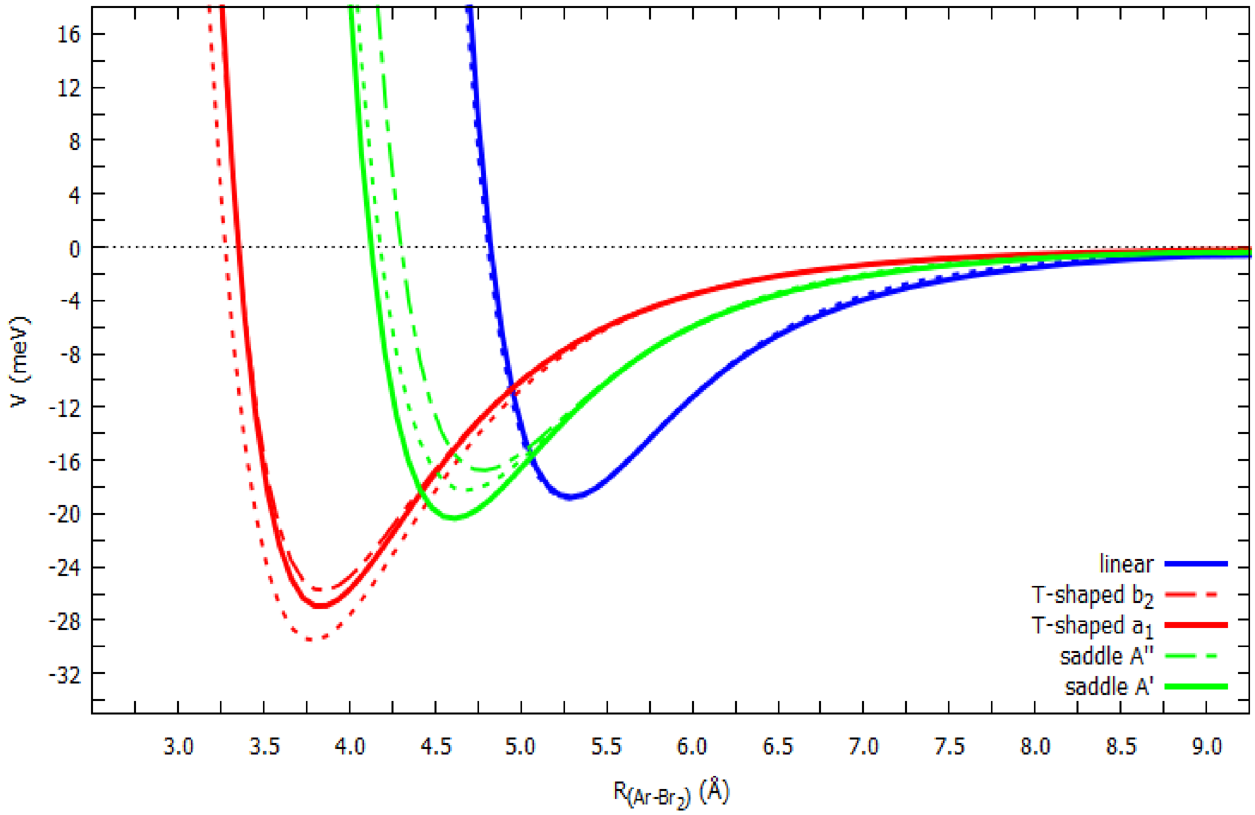

Figure 5. Potential energy curves (interaction potential V vs. Ar-Br$_2$ distance R) for the Ar-Br$_2$ system, with the Br$_2$ moiety in the ($B\ ^3\Pi_u$) excited state, computed at CCSD(T)/AV5Z level of theory (solid and dotted-dashed lines) and calculated with the semi-empirical method (dotted lines).

2.4 Halogen Polar Flattening in the Ng-X$_2$ complexes

A fundamental enabling feature of the XB is the so-called σ-hole on the halogen atoms, the axial electron deficiency which permits an approaching donor to bind. Associated with the σ-hole is a flattening of the halogen electron density on the outer side of the X$_2$ molecule along the bond direction. Remarkably, the strong anisotropy of the halogen electron density in the X$_2$ molecule can be related to a shift at lower distances of the repulsive wall, thus favouring a closer approach of the incoming Ng interacting partner in the linear configuration and rationalizing the higher energy stability of the linear vs T-shaped isomer. It is therefore highly desirable a rough estimation of the polar flattening in the X$_2$ series, also enabling a fine calibration of the semi-empirical parameters in the analytical potential form. One possibility consists in the comparison of the electron density profile of the X_2 molecules along two selected directions, namely the X_2 bond axis and the plane perpendicular to it, at the fixed X nucleus position. The results are reported in Figure 6, focusing on the low electron density regions, in the outermost part of halogens, which are of interest of the polar flattening. For each di-halogen molecule, the electron density profile along the bond axis direction is systematically lower than that along the direction perpendicular to it, thus confirming the polar flatting of the electron density for each halogen atom in the X_2 molecule. It is reasonable that the shift in the position of the repulsive wall in the linear isomers has to be strictly related to the shift at lower distance of the electron density profile along the X_2 bond vs the plane perpendicular to it. A measure of the shift may be provided by the Δz value, defined as the distance between two points of X_2 density profiles at a selected density value. At the isodensity value of 1 me/bohr^3, that is usually employed to map the Coulomb potential for the analysis of the σ-hole [18, 19], the Δz values are computed 0.23/0.25/0.25 Å for Cl_2/Br_2/I_2, thus suggesting a comparable flattening of the electron density on the outer region of the covalent bond in the halogen series. The estimated polar flattening enables a decrease at shorter distances of the repulsive wall position in the linear vs T-shaped isomer of about 4-5 %.

Peer-reviewed version available at *Molecules* **2019**, *24*, 4274; doi:10.3390/molecules24234274

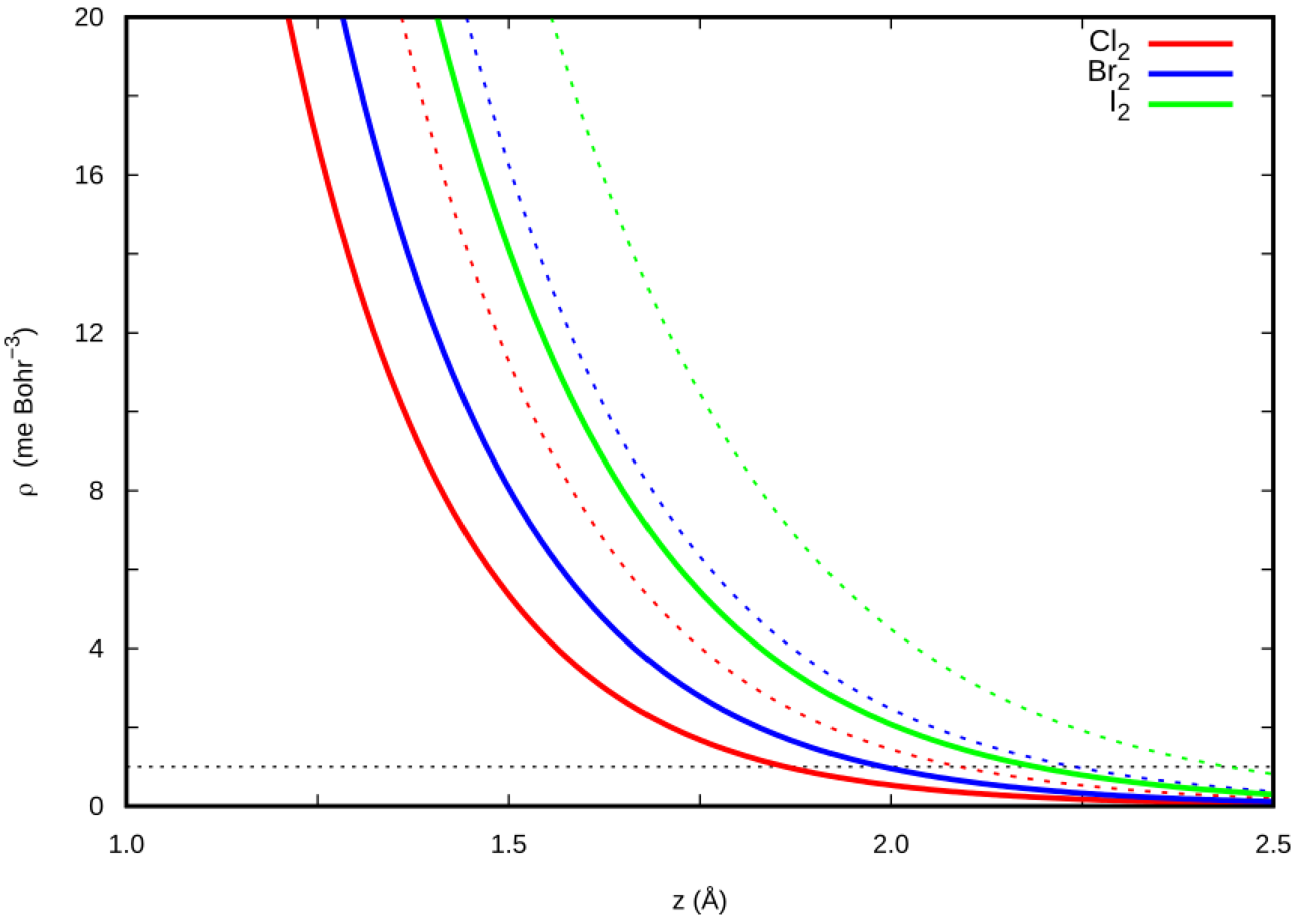

Figure 6. X_2 electron density profile, ρ (me·Bohr^{-3}), on the outer side of the X_2 molecule along the X_2 bond (solid lines) and perpendicular to it at the X nucleus (dotted lines).

2.5 Charge Displacement Analysis

The next subsection is addressed to the characterization of the dependence of CT on the basic physical properties of involved partners. This effort could be crucial to obtain a formulation of its stabilization contribution as far as of general validity. As previously done in the framework of our fine-tuned integrated experimental and theoretical approach [11-13], the presence of a CT component in the Ng-X_2 bond, that is required by the PES model to quantitatively reproduce the experimental cross sections, has been ascertained by resorting to the so-called CD function,[20] which has revealed especially useful for the identification and estimation of the CT in weakly bound systems [20-23]. The CD curves for selected Ng-X_2 (X = Br, I) systems in the linear configuration are reported in Figure 7, together with the 3D contour plots of the electron density

Peer-reviewed version available at *Molecules* **2019**, *24*, 4274; doi:10.3390/molecules24234274

difference between the complex and the non-interacting fragments. The X_2 substrate pronouncedly polarizes the spherical cloud of the Ng centre, which undergoes a depletion/accumulation in the region opposite / towards X_2. A visible amount of charge rearrangement is present even on the X_2 moiety. Moreover, the CD curves are distinctly positive everywhere, indicating a corresponding electron charge flow in the direction from Ng to X_2. This effect is a clear fingerprint of a donor role of Ng and is related to the presence of an XB interaction in the Ng-X_2 complexes. Remarkably both the σ-hole and the electron density polar flattening on the halogen concur to strengthen the CT in the linear isomer. For a plausible quantitative estimate of the amount of CT, we may take, as we have consistently done in previous works, the Δq value at the so-called "isodensity boundary", i.e. the point on z-axis where the electron densities of the non-interacting fragments become equal. The results are detailed in the top left inset of Figure 7, and yields comparable CT values for the Br_2 and I_2 complexes, ranging between 0.5 and 5.6-7.6 millielectron (me), going from the lighter to the heavier Ng. A similar trend has been encountered for the Ng-Cl_2 complexes (Ng = He, Ne, Ar) [11].

The CD analysis has been also carried out on the selected Ar-Br_2 complexes involving the Br_2 molecule in the excited $B\ {}^3\Pi_u$ state, showing that the CT is essentially negligible, as already discussed for the Ng-Cl_2 complexes [11].

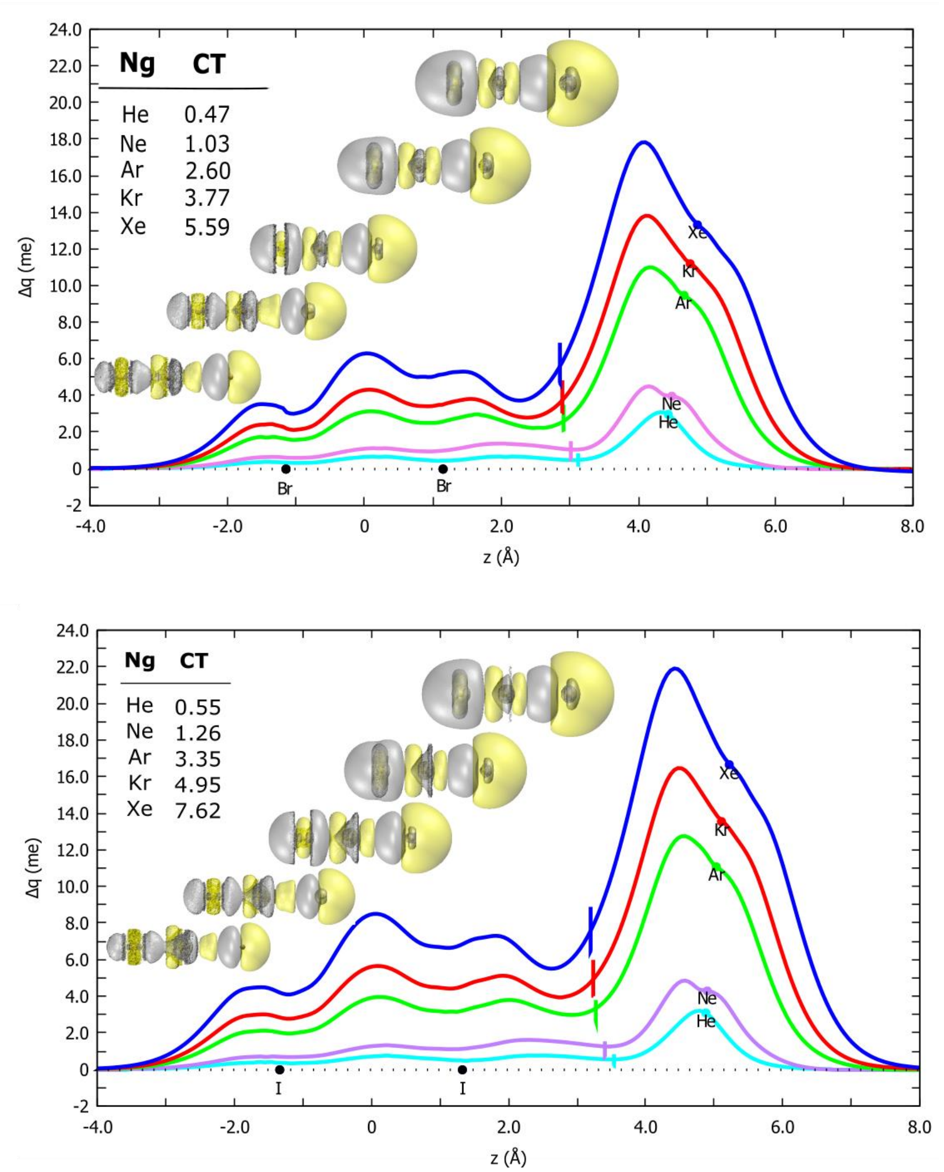

Figure 7. CD curves of ($X\ ^1\Sigma_g^+$) Ng-Br$_2$, top, and Ng-I$_2$, bottom, complexes in the linear configuration - dots represent the atomic nuclei position on the z-axis and vertical lines mark the isodensity boundaries. Inset: 3D isodensity plots of the electron density change, accompanying bond formation ($\Delta\rho=8\cdot10^{-6}$ me·Bohr^{-3}, negative/positive values in yellow/silver); CT values evaluated at the isodensity boundary.

2.6 CT Dependence on the First Ionization Potential

A proper rationalization of the increasing CT values along the Ng and X_2 series in terms of the properties of the involved fragments is highly desirable, since the interaction CT component plays a key role in the determination of differences in the energy stability among the various conformers. We expect that the CT (and, consequently, the related energy amount, V_{CT}) must be depending on the extent of the overlap between involved atomic/molecular orbitals. The associated contribution is ruled also by the energy separation between the states of the system coupled by CT. These effects can be modeled in terms of donor ionization energy and acceptor electron affinity, as they concur to determine both the dependence on the distance of the overlap integral, and of the separation energy between states of the system coupled by CT [24, 25]. Taking into account that present systems, as many other weakly bounded adducts, are affected by a non resonant CT couplings, considered in the perturbation limit [24], a meaningful general relation, defining strength and range of the V_{CT} component may be expressed as follows:

$$V_{CT}(\mathrm{R}) = \frac{B_X}{I_{Ng} - A_X - \frac{q^2}{R}} \cdot e^{-0.512\cdot\left(\sqrt{I_{Ng}}+\sqrt{A_X}\right)\cdot R} \qquad (1)$$

For the present systems, I_{Ng} is the donor first ionization energy and A_X is the electron affinity of the electrophile X_2. The numerator is correlated to the value of overlap integral between Ng and X_2 orbitals, and, in particular, the pre-exponential term, B_X, returns information on the size of the X_2 electron charge distribution. The denominator provides an estimate of the radial dependence of the energy difference between states coupled by CT, with the $(I_{Ng} - A_X)$ term being the energy separation between the Ng-X_2 and the Ng^+-X_2^- asymptotic energy, and the $\frac{q^2}{R}$ accounting for the Coulomb attraction between Ng^+ and X_2^- at the distance R

It is quite instructive to compare the behavior of V_{CT}, provided by Eq. 1, with that gained from the semiempirical model, see Eq. 9 (see section 3), for three series of Ng-X_2 systems in the collinear

Peer-reviewed version available at *Molecules* **2019**, *24*, 4274; doi:10.3390/molecules24234274

configuration. In all cases V_{CT} has been evaluated at a selected intermediate distance value of R=3 Å, here representing the separation distance between the Ng center and the X atom closer to Ng, being the only effectively involved in the CT from Ng to X_2. The use of such condition is suitable to emphasize the V_{CT} dependence on basic properties of the partners. Adopting Eq.1, the B_X parameter has been optimized in order to obtain the best comparison with the reference V_{CT} contribution (also including the model uncertainties) gained from the semi-empirical parametrization (see below).

In the comparison we also included the Ng-Cl adduct, which was previously investigated through state selected Cl atom beam experiments, carried out with the same molecular beam apparatus used here [24]. We report, in Table 3, the optimized parameters for the V_{CT} formula (Eq. 1), together with the I_{Ng} and A_X values, as taken from the literature.

Table 3. Ng first ionization potential energies (I_{Ng}), X/X_2 electron affinities (A_X) and B_X optimized parameters.

	I_{Ng} (eV)(a)		A_X (eV)(a)	B_X [$(\mathrm{eV})^2$](b)
He	24.587	**Cl**	3.621	3430
Ne	21.564	**Cl_2**	2.38 ± 0.1	1300
Ar	15.759	**Br_2**	2.55 ± 0.1	2500
Kr	13.999	**I_2**	2.55 ± 0.05	5000
Xe	12.130			

(a) Values from reference [26]; (b) Absolute error of ±10%.

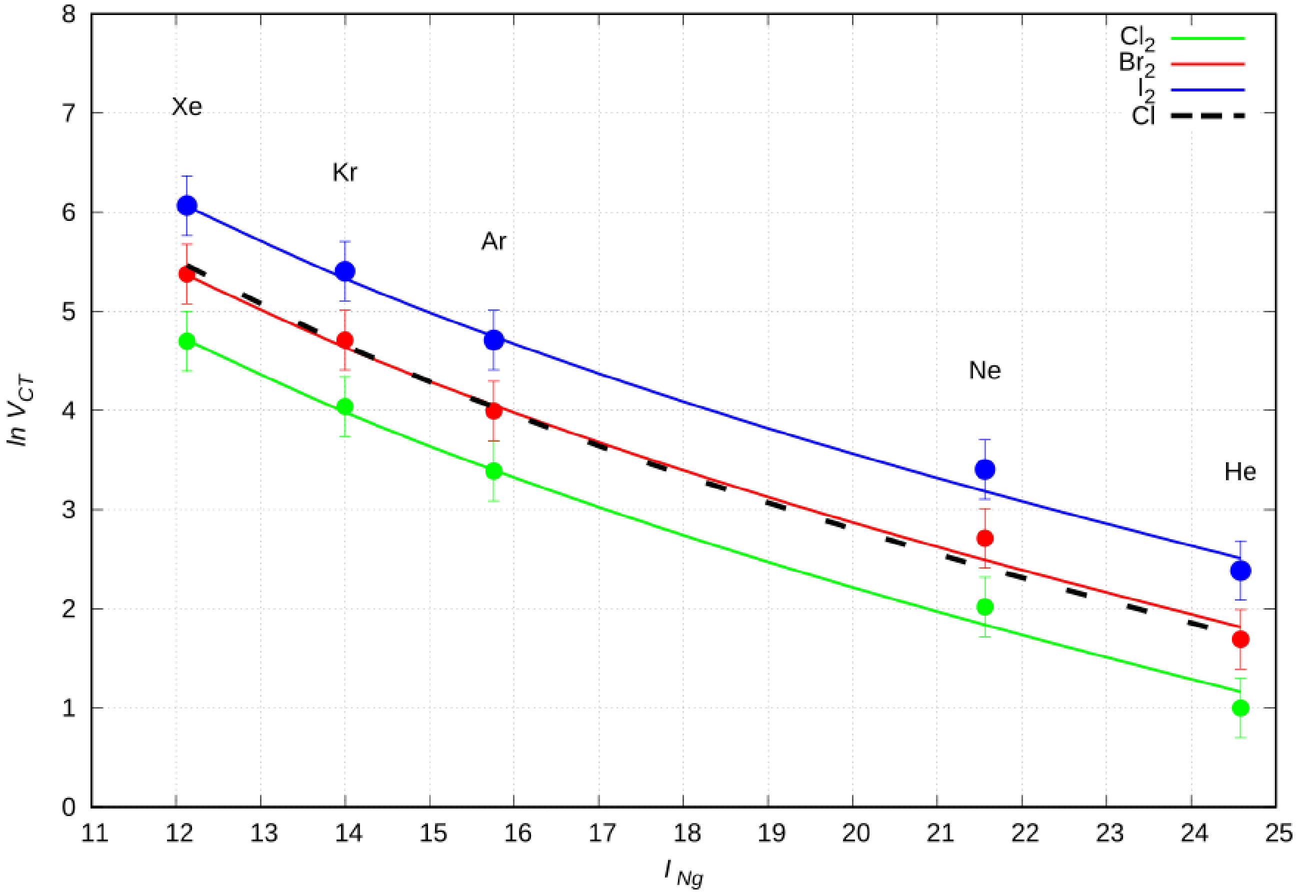

Figure 8. *Ln* V_{CT} in the Ng-X$_2$ complexes linear configurations vs. Ng first ionization energy (I_{Ng}, eV). Solid lines identify the values derived from Eq. 1, while symbols with error bars refer to Eq. 9; the dashed line refer to the Ng-Cl system.

From Figure 8, we notice that the semi-empirical function (Eq. 1) reproduces, within the error range, the calculated V_{CT} values, suggesting the following trend: Ng-Cl$_2$ < Ng-Cl ≃ Ng-Br$_2$ < Ng-I$_2$. This behavior can be explained introducing the V_{CT} dependence on the di-halogens dimension and electronic affinities: more they are electrophiles, more their V_{CT} component is high. For the Cl atom, we have a different electronic deficit, because it has, properly, an electron missing on the *3p* orbital.

Peer-reviewed version available at Molecules 2019, 24, 4274; doi:10.3390/molecules24234274

2.7 CT Proportional Constant

As a final important aspect of the CT component, contributing to the formation of the weak intermolecular XB, we briefly discuss the relation between the amount of charge transferred and the energy stabilization of the adduct arising from this interaction component. It is clear that, when CT is sufficiently small, as it is in the present cases, we should expect the energy stabilization V_{CT} to be roughly proportional to CT, that is: $V_{CT} = k \cdot \mathrm{CT}$. Wang et al. [27] have indeed found an excellent linear correlation. Obtaining a reliable estimate of the energy stabilization per transferred charge unit (*k*) is clearly a result of general interest, and the employed phenomenological-theoretical approach enables to do just that.

We have evaluated the *k* value for each Ng-X_2 system in the collinear isomer as the ratio between the V_{CT} strength, as predicted by the semiempirical model at the *ab initio* optimized equilibrium distance, and the *ab initio* CT quantity. The results, with their appropriate error bars, are shown in Figure 9 for the whole series of Ng elements, displayed on the scale of their ionization energy. The average proportional constant results $(4.6 \pm 1.0)\mathrm{eV/e}$, with the associated global error being estimated considering the combined uncertainty in the V_{CT} (pre-exponential factor A_{CT} has a 15% error) and in the separation between the polar flattening and the CT stabilization contributions.

Peer-reviewed version available at Molecules 2019, 24, 4274; doi:10.3390/molecules24234274

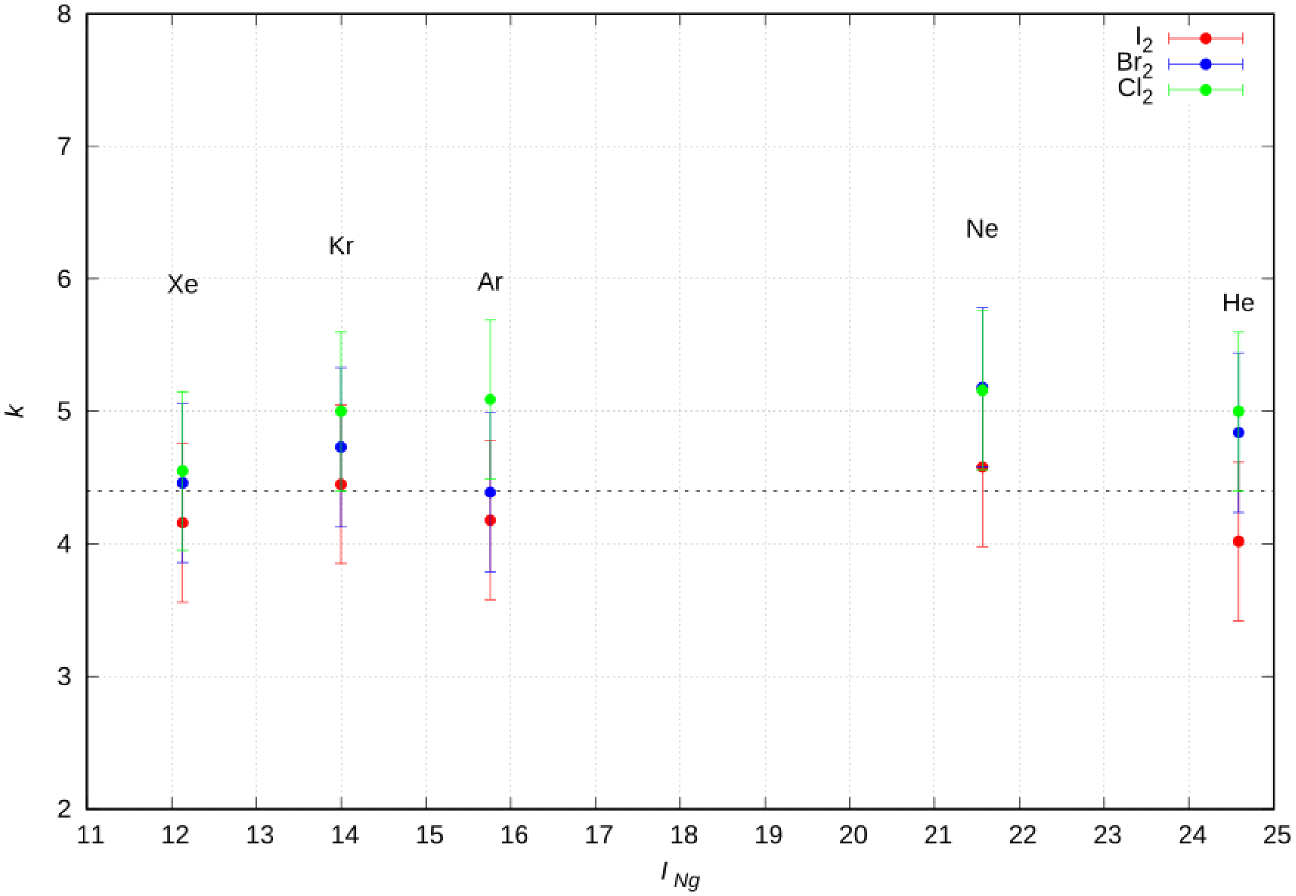

Figure 9. k values for each Ng-X_2 system in the collinear isomer gained as ratio between the V_{CT} strength, predicted by the semiempirical model at the *ab initio* optimized equilibrium distance, and the *ab initio* CT quantity, vs. the Ngs first ionization energy (I_{Ng}, eV).

3. Materials and Methods

3.1 Phenomenological approach

The phenomenological approach is solidly founded on the experiments carried out with the molecular beam technique, using the He, Ne and Ar noble gases as projectiles and the electronic ground state Cl_2 / Br_2 halogen molecules as targets. At given angle and energy resolution conditions, we measure the total integral cross-section $Q(v)$ as a function of the collision velocity v, so that quantum "glory" interference effects are resolved. Unfortunately, on the present experimental apparatus, limit-angle problems prevent the measurement of the true quantum cross-section for

Peer-reviewed version available at Molecules 2019, 24, 4274; doi:10.3390/molecules24234274

heavier Kr or Xe beams. Similarly, substantial modifications of the apparatus and different operative conditions would be required to enable experiments with I_2 targets.

Using the results from the measured integral cross-section *Q(v)* as a function of the collision velocity *v* (see Figure 1), integrated with other experimental data on various types of weakly bounded interacting systems, we propose a well-defined and simple formulation of the intermolecular potential in the Ng-X_2 systems. By denoting with *R* the distance of the Ng atom from the midpoint of the X_2 bond (the latter assumed of fixed length) and with θ the angle between **R** and the X_2 bond axis (see Figure S1 in the SM), this formulation reads:

$$V(R, \Theta) = V_{vdW}(R, \Theta) + V_{3B}(R, \Theta) + V_{CT}(R, \Theta) \qquad (2)$$

As previously ascertained, V_{vdW} is best represented as the sum of individual interactions between Ng and each of the two X atoms (X_a and X_b), $V_{vdW} = V_{Ng\text{-}X_a} + V_{Ng\text{-}X_b}$, each of them expressed as an Improved Lennard-Jones (ILJ) function of the distance r_i between Ng and X_i and of the angle φ_i between $\mathbf{r}_i$ and the X_2 axis (see Figure S1):

$$V_{Ng-X_i}(r_i, \varphi_i) = \varepsilon(\varphi_i)\left[\frac{6}{n(r_i,\varphi_i)} \cdot \left(\frac{r_m(\varphi_i)}{r_i}\right)^{n(r_i,\varphi_i)} - \frac{n(r_i,\varphi_i)}{n(r_i,\varphi_i)-6} \cdot \left(\frac{r_m(\varphi_i)}{r_i}\right)^{6}\right] \qquad (3)$$

Here, the $\varepsilon(\varphi_i)$ and $r_m(\varphi_i)$ parameters (potential energy minimum and equilibrium distance, respectively) are calculated as follows:

$$\varepsilon(\varphi_i) = \varepsilon_{||} \cdot cos^2(\varphi_i) + \varepsilon_{\perp} \cdot sin^2(\varphi_i) \qquad (4)$$

$$r_m(\varphi_i) = r_{m||} \cdot cos^2(\varphi_i) + r_{m\perp} \cdot sin^2(\varphi_i) \qquad (5)$$

where the || and ⊥ symbols refer to the collinear ($\varphi_i = 0$) and perpendicular ($\varphi_i = \pi/2$) configurations, respectively. The factor $n(r_i, \varphi_i)$, which modulates the fall-off of the repulsion and the radial dependence of the intermediate and long-range attraction, depends on β, an additional parameter related to the "hardness" of the interacting partners, as follows:

Peer-reviewed version available at Molecules 2019, 24, 4274; doi:10.3390/molecules24234274

$$n(r_i, \varphi_i) = \beta + 4 \cdot \left(\frac{r_i}{r_m(\varphi_i)}\right)^2 \qquad (6)$$

Here β is optimally found to lie in the interval 7.0-7.5 for all atom pairs. The partial long-range dispersion attraction coefficients are described only by the asymptotic V_{vdW} component of the potential and, according to the ILJ formulation, their expression is:

$$C_{6i} = \left[\varepsilon(\varphi_i) \cdot r_m^6(\varphi_i)\right] \qquad (7)$$

with the global attraction coefficient resulting as the sum of the two angularly averaged C_{6i} terms.

The values of the ε and the r_m parameters have been predicted in an internally consistent way for all Ng-X_2 systems from the polarizability components (See refs 10-14 and references therein) and they have been validated by comparing the calculated cross-sections with the experimental results. During the analysis, an additional constraint of providing global average asymptotic attractions has been imposed in order to obtain a satisfactory agreement (within about 10%) with the results reported in reference [28].

As previously done for other systems involving halogen atoms [11, 29, 30], the zero order values of $r_{m||}$ have been decreased by about 4% to account for the polar flattening effect in the ground state of X_2. Such effect is related to the peculiarity of the electronic charge distribution of the X atom in the direction pointing at the approaching Ng atom in the collinear isomer, the origin and details of which are rationalized in the theoretical sections of this paper. The reduction of $r_{m||}$ must be accompanied by corresponding increase of $\varepsilon_{||}$ in order to maintain the C_6coefficient constant.

The second term, V_{3B}, in the expression for $V(R, \Theta)$, can be conveniently formulated as:

$$V_{3B}(R, \Theta) = A_{3B} \cdot sin^2(2\Theta) e^{-3.0 \cdot R} \qquad (8)$$

This term is crucial to properly represent the angular dependence of the full PES, especially in the proximity of the saddle point between the collinear and perpendicular configurations, where the molecular repulsion by occupied π* orbitals is more prominent. With respect to a previous

Peer-reviewed version available at Molecules 2019, 24, 4274; doi:10.3390/molecules24234274

formulation [11], the expression for this term has been slightly improved to guarantee a smooth second derivative in vicinity of $\Theta = \pi/2$.

Finally, the charge-transfer term of the potential formulation has been defined as:

$$V_{CT}(R,\Theta) = -\sum_{i=a,b} A_{CT} \cdot cos^4(\varphi_i) \cdot e^{-3.0 \cdot r_i} \quad (9)$$

The dynamical treatment used for the scattering data analysis has been extensively described in recent papers. It affords a satisfactory reproduction of the measured $Q(v)$ (full lines in Figure 1) by essentially only varying the parameters A_{3B} and A_{CT}, while keeping the other parameters fixed at their predicted value to within very small adjustments.

The modulation of the involved potential parameters is gained through empirical/semi-empirical formulas developed in our laboratory [10-14,27,28], which represent the strength of the basic intermolecular interaction components in terms of fundamental physical properties of the involved partners, such as the electronic polarizabilities, which define strength, range and anisotropy of the V_{vdW} component. Such formulas also account for the dependence of specific parameters on the ionization potential of Ng and on the $\pi^* \longrightarrow \sigma^*$ electronic excitation of X_2, which is accompanied by a substantial electronic charge rearrangement, causing an increase of the molecular polarizability and of its anisotropy.

By then comparing the model predictions with the results of *ab initio* calculations, reported in the previous section, the potential parameters can be further refined and thereby the overall potential formulation exhaustively validated for the entire family of Ng-X_2 adducts, with X_2 either in its ground or first excited electronic state. The parameters values derived for the analytical form of the Ng-X_2 PESs are reported in Tables 4-5.

Peer-reviewed version available at *Molecules* **2019**, *24*, 4274; doi:10.3390/molecules24234274

Table 4. Potential parameters (r_m in Å; ε, A_{CT}, A_{3B} in meV) employed for the formulation of the Ng-Cl atom-atom pairwise interaction for Ng-X_2 systems in the ($X\ {}^1\Sigma_g^+$) ground state. || and ⊥ symbols refer to the collinear and perpendicular configurations. β is equal to 7.0 except for Ng-Cl_2 systems (β=7.5). The maximum estimated uncertainty is about 10% for ε,, 3% for r_m and 10-15% A_{CT} and A_{3B}.

	$r_{m\parallel}$	$\varepsilon_\parallel$	$r_{m\perp}$	$\varepsilon_\perp$	A_{CT}	A_{3B}
He-Cl₂	3.39	4.47	3.55	2.93	310000	22000
Ne-Cl₂	3.44	8.76	3.60	5.76	450000	61000
Ar-Cl₂	3.68	19.70	3.85	13.00	700000	240000
Kr-Cl₂	3.79	24.40	3.98	15.70	830000	460000
Xe-Cl₂	3.94	28.20	4.14	18.10	970000	890000
He-Br₂	3.53	4.71	3.71	3.02	620000	44000
Ne-Br₂	3.57	9.66	3.75	6.21	900000	120000
Ar-Br₂	3.80	21.30	4.00	13.90	1400000	440000
Kr-Br₂	3.87	28.90	4.07	18.40	1660000	900000
Xe-Br₂	4.01	34.50	4.23	21.90	1900000	1750000
He-I₂	3.81	4.00	4.06	2.59	1550000	88000
Ne-I₂	3.81	8.76	4.05	5.70	2250000	244000
Ar-I₂	3.95	23.60	4.20	15.50	3500000	900000
Kr-I₂	4.03	30.90	4.28	20.30	4150000	1800000
Xe-I₂	4.16	38.60	4.41	25.60	4750000	3500000

Peer-reviewed version available at *Molecules* **2019**, *24*, 4274; doi:10.3390/molecules24234274

Table 5. Potential parameters (r_m in Å; ε, A_{CT}, A_{3B} in meV) employed for the formulation of the Ng-Cl atom-atom pairwise interaction for Ng-X_2 systems in the ($B^3\Pi_u$ $^+$) excited state. ‖ and ⊥ symbols refer to the collinear and perpendicular configurations. β is equal to 7.0 except for Ng-Cl_2 systems (β=7.5). The maximum estimated uncertainty is about 10% for ε and 3% for r_m.

	$r_{m\parallel}$	$\varepsilon_\parallel$	$r_{m\perp}$	$\varepsilon_\perp$	A_{CT}	A_{3B}
He-Cl$_2$	3.62	3.03	3.58	2.88	0	0
Ne-Cl$_2$	3.64	6.32	3.62	5.73	0	0
Ar-Cl$_2$	3.81	16.30	3.87	13.40	0	0
Kr-Cl$_2$	3.91	20.90	3.98	16.70	0	0
Xe-Cl$_2$	4.06	25.70	4.14	19.80	0	0
He-Br$_2$	3.83	2.92	3.81	2.66	0	0
Ne-Br$_2$	3.83	6.27	3.83	5.53	0	0
Ar-Br$_2$	3.96	17.70	4.02	14.40	0	0
Kr-Br$_2$	4.04	23.30	4.11	18.60	0	0
Xe-Br$_2$	4.16	29.60	4.26	22.60	0	0
He-I$_2$	4.12	2.70	4.12	2.40	0	0
Ne-I$_2$	4.09	6.00	4.11	5.20	0	0
Ar-I$_2$	4.16	19.00	4.23	15.40	0	0
Kr-I$_2$	4.23	25.80	4.31	20.60	0	0
Xe-I$_2$	4.33	34.30	4.42	26.60	0	0

3.2 Computational Details

The *ab initio* calculations have been performed with the MOLPRO program [31]. Since the investigated non-covalent interactions have a strong dispersion component, it is fundamental that the computational method used to treat a HX system is of highly accurate level, adequately accounting for the consistent electron correlation. Accordingly, the calculations have been carried out at the coupled-cluster level of theory [32], with single, double and perturbatively included triple excitations, CCSD(T), using augmented correlation consistent polarized valence triple- (only in the

Peer-reviewed version available at Molecules 2019, 24, 4274; doi:10.3390/molecules24234274

He case), quadruple-, quintuple-ζ basis sets, (aug-cc-PVXZ, hereafter labelled as AVXZ, with X=T, Q, 5). Selected cuts of the ground state PESs for the Ng-X_2 (X = Br, I) complexes were investigated by considering the Ng atom in the $^1S_0$ ground state and the Cl_2 molecule in the ($X^1\ \Sigma_g^+$) ground state. We also considered the Ar-Br_2 complex with Br_2 being in its first excited state ($B^3\Pi_u$), characterized by a $(\pi_g^*)^3(\sigma_u^*)^1$ valence shell configuration. Remarkably, the double degeneracy of the Π state is lifted upon approach of the Ng atom. The overall symmetry is lowered to the C_{2v} (C_s) point groups for the T-shaped (saddle) isomer, and leads to two electronic states with A_1 / B_2 (A' / A'') symmetries, which become degenerate for the collinear geometry.

According to the formulation of the phenomenological PES, we used the Jacobi coordinates (R, r, Θ) to describe the triatomic Ng-X_2 complexes. The Br-Br (I-I) bond distance in the adducts has been fixed at the equilibrium value 2.28 Å (2.666 Å) in the isolated Br_2 (I_2) molecule in the ground state [33], since the relatively weak interaction with Ng is expected to leave the geometry of X_2 essentially unaffected. For the Br_2 molecule first excited state an equilibrium distance of 2.699 Å has been considered [34]. For each Ng-X_2 complex, we varied the intermolecular distance, R in the range 2.0-7.0 Å, for both $\Theta = 0°$ and 90° values. For the X ground state, we also examined peculiar cuts of the Ng-X_2 PESs by varying the Θ angle in the range 0 - 90° (step by 5°) and optimizing the intermolecular distance R. In this case, the Θ value corresponding to the energy maximum along the path returns the saddle configuration between the two limiting ones.

The basis set superposition errors (BSSEs) on the interaction energy values computed with the AVXZ basis sets have been evaluated by applying the counterpoise method [35, 36].

3.3 Charge Displacement Function

As the above discussion implies, specific configurations of Ng-X_2 (X = Br, I) may be selectively stabilized when there is a CT component. A well-established method that permits in a simple yet powerful way to access and quantify the electron displacement occurring upon formation of the

Peer-reviewed version available at Molecules 2019, 24, 4274; doi:10.3390/molecules24234274

bond, is the CD function [20]. This function gives, at each point z along an axis joining two interacting fragments, the electron charge (Δq) that, upon formation of the complex, has been displaced from right to left across the plane perpendicular to the axis through z. Its expression is:

$$\Delta q(z) = \int_{-\infty}^{+\infty} dx \int_{-\infty}^{+\infty} dy \int_{-\infty}^{z} \Delta\rho(x,y,z')dz' \qquad (10)$$

Where the integrand $\Delta\rho$ is the electron density difference between the complex under study and its non-interacting fragments, i.e. the change in electron density brought about by the interaction.

The CD curve provides in most cases a straightforward and unambiguous tool to assess the presence and extent of CT in the formation of the adduct, especially in few-atoms systems such as the ones at hand. If the function is appreciably different from zero and does not change in sign in the region between the fragments, we can with confidence assert that CT is taking place. Conversely, if the curve crosses zero in this region, CT may be uncertain (both in magnitude and direction). When CT is ascertained, it is useful, for comparative purpose, to obtain a definite numerical estimate of it, by considering the CD function value at a specific point between the fragments along the z axis. In this case, as in previous ones [11-13], we chose as fragment separator the point along z at which the electron densities of the non-interacting fragments become equal (*isodensity boundary*).

4. Conclusions

In the present manuscript we have characterized by a thoroughly integrated experimental and theoretical approach the XB interaction in the series of prototype noble gas – dihalogen adducts. We gain an internally consistent description for the interaction in all the Ng-X_2 families (Ng = He, Ne, Ar, Kr, Xe; X_2 = Cl_2, Br_2, I_2), together with an analytical formulation of all the PESs, that is fine tuned by few well-defined physical parameters. The nature of the interaction is strongly anisotropic not only in the X_2 ground state, but also for the excited one. In the Ng-X_2 ground state an interaction with XB characteristic clearly emerges limited to the linear configuration, as suggested by the polar flattening of the X_2 electron density along the X-X bond direction and by the presence

Peer-reviewed version available at *Molecules* **2019**, *24*, 4274; doi:10.3390/molecules24234274

of a sizable CT accompanying the adduct formation. These peculiar features are missing in the T-shape orientation adducts or in the linear complexes involving the X_2 excited state, so that the interaction has substantially a vdW nature. The analytical potential formulation based on the investigated prototype Ng-X_2 adducts can be easily extended to more complex systems, such as those involving the H_2O or NH_3 polyatomic molecules as interacting partners. Remarkably, in the latter cases a more pronounced anisotropy character is expected in the XB interaction, being affected by the interacting partner orientation.

Author Contributions: Investigation, B.D. and D.C.; Methodology, F.P.; Visualization, F. N. and D. C.; Writing – original draft, F.N., F. T. and F. P.; Writing—review and editing, F.N and F.P.

Acknowledgements: The authors acknowledge support from the Ministero Istruzione dell’Università e della Ricerca (MIUR) and the University of Perugia through the program “Dipartimenti di Eccellenza 2018-2022” (grant AMIS). They also thank the University of Perugia for funding through the “Fondo Ricerca di Base 2017” programme.

Conflicts of Interest: The authors declare no conflict of interest.

References

[1] G.R. Desiraju, P.S. Ho, L. Kloo, A.C. Legon, R. Marquardt, P. Metrangolo, P. Politzer, G. Resnati, K. Rissanen, Definition Of The Halogen Bond (IUPAC Recommendations 2013), Pure Appl. Chem., 85 (2013) 1711-1713.
[2] Z.M. Han, G. Czap, C.L. Chiang, C. Xu, P.J. Wagner, X.Y. Wei, Y.X. Zhang, R.Q. Wu, W. Ho, Imaging The Halogen Bond In Self-Assembled Halogenbenzenes On Silver, 358 (2017) 206-210.
[3] L.C. Gilday, S.W. Robinson, T.A. Barendt, M.J. Langton, B.R. Mullaney, P.D. Beer, Halogen Bonding in Supramolecular Chemistry, Chem. Rev., 115 (2015) 7118-7195.
[4] A. Rohrbacher, N. Halberstadt, K.C. Janda, The Dynamics of Noble Gas-Halogen Molecules and Clusters, Annu. Rev. Phys. Chem., 51 (2000) 405-433.
[5] J.A. Beswick, N. Halberstadt, K.C. Janda, Structure and Dynamics of Noble Gas-Halogen and Noble Gas Ionic Clusters: When Theory Meets Experiment, Chem. Phys., 399 (2012) 4-16.
[6] J. Wei, C. Makarem, A.L. Reinitz, J.P. Darr, R.A. Loomis, Accurate Measurement Of The T-Shaped And Linear Ar··· $I_2(X, \nu''=0)$ Binding Energies Using Vibronic-Specific $I_2(B, \nu)$ Fragment Velocity-Map Imaging, Chem. Phys., 399 (2012) 172-179.
[7] L. Delgado-Tellez, A. Valdes, R. Prosmiti, P. Villarreal, G. Delgado-Barrio, Ab Initio Characterization Of The Ne-I_2 Van Der Waals Complex: Intermolecular Potentials And Vibrational Bound States, J. Chem. Phys., 134 (2011).
[8] V.V. Baturo, S.S. Lukashov, S.A. Poretsky, A.M. Pravilov, The RgI_2 (Ion-Pair States) van der Waals Complexes, Eur. Phys. J. D, 71 (2017) 227.

[9] A.C. Legon, The Halogen Bond: an Interim Perspective, Phys. Chem. Chem. Phys., 12 (2010) 7736-7747.
[10] F. Pirani, D. Cappelletti, S. Falcinelli, D. Cesario, F. Nunzi, L. Belpassi, F. Tarantelli, Selective Emergence of Halogen Bond in Ground and Excited States of Noble-Gas—Chlorine Systems, Angew. Chem. Int. Ed., 58 (2019) 4195-4199.
[11] F. Nunzi, D. Cesario, L. Belpassi, F. Tarantelli, L.F. Roncaratti, S. Falcinelli, D. Cappelletti, F. Pirani, Insight Into The Halogen-Bond Nature Of Noble Gas-Chlorine Systems By Molecular Beam Scattering Experiments, Ab Initio Calculations And Charge Displacement Analysis, Phys. Chem. Chem. Phys., 21 (2019) 7330-7340.
[12] M. De Santis, F. Nunzi, D. Cesario, L. Belpassi, F. Tarantelli, D. Cappelletti, F. Pirani, Cooperative Role Of Halogen And Hydrogen Bonding In The Stabilization Of Water Adducts With Apolar Molecules, New J. Chem., 42 (2018) 10603-10614.
[13] D. Cappelletti, V. Aquilanti, A. Bartocci, F. Nunzi, F. Tarantelli, L. Belpassi, F. Pirani, Interaction of O_2 with CH_4, CF_4, and CCl_4 by Molecular Beam Scattering Experiments and Theoretical Calculations, J. Phys. Chem. A, 120 (2016) 5197-5207.
[14] D. Cappelletti, E. Ronca, L. Belpassi, F. Tarantelli, F. Pirani, Revealing Charge-Transfer Effects in Gas-Phase Water Chemistry, Acc. Chem. Res., 45 (2012) 1571-1580.
[15] D. Cappelletti, A. Cinti, A. Nicoziani, S. Falcinelli, F. Pirani, Molecular Beam Scattering Experiments as a Sensitive Probe of the Interaction in Bromine-Noble Gas Complexes, Front. Chem., 7 (2019) 10.
[16] F. Pirani, F. Vecchiocattivi, A Fast And Accurate Semiclassical Calculation Of The Total Elastic Cross Section In The Glory Energy Range, Mol. Phys., 45 (1982) 1003-1013.
[17] F. Pirani, S. Brizi, L.F. Roncaratti, P. Casavecchia, D. Cappelletti, F. Vecchiocattivi, Beyond The Lennard-Jones Model: A Simple And Accurate Potential Function Probed By High Resolution Scattering Data Useful For Molecular Dynamics Simulations., Phys. Chem. Chem. Phys., 10 (2008) 5489-5503.
[18] T. Clark, M. Hennemann, J.S. Murray, P. Politzer, Halogen Bonding: the σ-hole, J. Mol. Model., 13 (2007) 291-296.
[19] K.E. Riley, J.S. Murray, J. Fanfrlik, J. Rezac, R.J. Sola, M.C. Concha, F.M. Ramos, P. Politzer, Halogen bond tunability II: the varying roles of electrostatic and dispersion contributions to attraction in halogen bonds, J. Mol. Model., 19 (2013) 4651-4659.
[20] L. Belpassi, I. Infante, F. Tarantelli, L. Visscher, The Chemical Bond Between Au(I) and the Noble Gases. Comparative Study of NgAuF And $NgAu^+$ (Ng = Ar, Kr, Xe) By Density Functional and Coupled Cluster Methods, J. Am. Chem. Soc., 130 (2008) 1048-1060.
[21] G. Bistoni, L. Belpassi, F. Tarantelli, F. Pirani, D. Cappelletti, Charge-Displacement Analysis of the Interaction in the Ammonia-Noble Gas Complexes, J. Phys. Chem. A, 115 (2011) 14657-14666.
[22] F. Nunzi, D. Cesario, F. Pirani, L. Belpassi, G. Frenking, F. Grandinetti, F. Tarantelli, Helium Accepts Back-Donation In Highly Polar Complexes: New Insights into the Weak Chemical Bond, J. Phys. Chem. Lett., 8 (2017) 3334-3340.
[23] F. Nunzi, D. Cesario, F. Pirani, L. Belpassi, F. Tarantelli, Modelling Charge Transfer in Weak Chemical Bonds: Insights from the Chemistry of Helium, ChemPhysChem, 19 (2018) 1476-1485.
[24] V. Aquilanti, D. Cappelletti, V. Lorent, E. Luzzatti, F. Pirani, The Ground And Lowest Excited-States Of XeCl By Atomic-Beam Scattering, Chem. Phys. Lett., 192 (1992) 153-160.
[25] F. Pirani, A. Giulivi, D. Cappelletti, V. Aquilanti, Coupling By Charge Transfer: Role In Bond Stabilization For Open-Shell Systems And Ionic Molecules And In Harpooning And Proton Attachment Processes, Mol. Phys., 98 (2000) 1749-1762.
[26] R.C. Weast, M.J. Astle, W.H. Beyer, CRC handbook of chemistry and physics, CRC press Boca Raton, FL1988.
[27] C. Wang, D. Danovich, Y. Mo, S. Shaik, On The Nature of the Halogen Bond, J. Chem. Theory Comput., 10 (2014) 3726-3737.
[28] T.N. Olney, N.M. Cann, G. Cooper, C.E. Brion, Absolute scale determination for photoabsorption spectra and the calculation of molecular properties using dipole sum rules, Chem. Phys., 223 (1997) 59-98.
[29] D. Cappelletti, A. Bartocci, F. Grandinetti, S. Falcinelli, L. Belpassi, F. Tarantelli, F. Pirani, Experimental Evidence of Chemical Components in the Bonding of Helium and Neon with Neutral Molecules, Chem. Eur. J., 21 (2015) 6234-6240.

Peer-reviewed version available at *Molecules* **2019**, *24*, 4274; doi:10.3390/molecules24234274

[30] A. Bartocci, L. Belpassi, D. Cappelletti, S. Falcinelli, F. Grandinetti, F. Tarantelli, F. Pirani, Catching the Role of Anisotropic Electronic Distribution and Charge Transfer in Halogen Bonded Complexes of Noble Gases, J. Chem. Phys., 142 (2015) 184304
[31] H.J. Werner, P.J. Knowles, G. Knizia, F.R. Manby, M. Schutz, Molpro: A General-Purpose Quantum Chemistry Program Package, Wiley Interdiscip. Rev. Comput. Mol. Sci., 2 (2012) 242-253.
[32] K. Raghavachari, G.W. Trucks, J.A. Pople, M. Headgordon, A 5th-Order Perturbation Comparison Of Electron Correlation Theories, Chem. Phys. Lett., 157 (1989) 479-483.
[33] K.P. Huber, G. Herzberg, Molecular Spectra and Molecular Structure, Constants of Diatomic Molecules, Vol. IV, Van Nostrand, New York, 1979.
[34] R.J. Le Roy, R.B. Bernstein, Dissociation Energies and Long-Range Potentials of Diatomic Molecules from Vibrational Spacings: The Halogens, J. Mol. Spectrosc., 37 (1971) 109-130.
[35] H.B. Jansen, P. Ros Non-Empirical Molecular Orbital Calculations on the Protonation of Carbon Monoxide., Chem. Phys. Lett., 3 (1991) 140-143.
[36] B. Liu, A.D. McLean, Accurate Calculation of the Attractive Interaction of Two Ground State Helium Atoms, J. Chem. Phys., 59 (1973) 4557-4558.